Coverage Analysis for Satellite Downlink Networks

Namyoon Lee
Department of Electrical Engineering
Korea University, Seoul, South Korea
namyoon@korea.ac.kr

ICC 2022 - IEEE International Conference on Communications | 978-1-5386-8347-7/22/$31.00 ©2022 IEEE | DOI: 10.1109/ICC45855.2022.9838263

***Abstract*—In this paper, we develop novel models that are tractable for the coverage and rates analysis using stochastic geometry. By modeling the locations of satellites and users using Poisson point processes (PPPs) on the surfaces of concentric spheres with distinct radii, we characterize analytical expressions for the coverage probability of a typical downlink user as a function of relevant parameters. Then, we also derive a tight lower bound of the coverage probability in closed-form expression while keeping full generality. Leveraging the derived expression, we identify the optimal density of satellites in terms of the altitude. Our key finding is that the required average number of satellites scales down logarithmically with the network height to maximize the coverage performance. Simulation results verify the exactness of the derived expressions.**

I. Introduction

Universal coverage is a persistent trend in wireless communications. Satellite networks integrated with terrestrial cellular networks can be promising solutions to provide seamless and ubiquitous connectivity services [1]. While classical satellite networks using geosynchronous equatorial orbit (GEO) are effective at providing stationary coverage to a specific area, the attention of researchers is recently shifting to satellite networks employing the low Earth orbit (LEO) or very LEO (VLEO) mega-satellite constellations. Unlike GEO satellite networks, LEO or VLEO satellite networks can achieve higher data rates with much lower delays at the cost of deploying more dense satellites to attain global coverage performance.

The characterization of the coverage and rate performance for VLEO satellite networks is of importance because of ultra-expensive costs for deploying mega VLEO satellites. Satellite networks are conventionally modeled by placing satellites on a grid of multiple circular orbit geometries, e.g., the Walker constellations. This model, however, is not very analytically tractable to characterize coverage and rate performance, so intricate system-level simulations are required to evaluate such performance by numerically averaging out the many sources of randomness, including satellites' locations and channel fadings. Stochastic geometry is a mathematical tool that characterizes the spatial distributions of base stations' and users' locations in wireless networks [3]. Significant progress has been made in recent years on characterizing wireless networks' coverage and rate performances using stochastic geometry. By modeling the placements of base stations and users according to Poisson point processes (PPPs), analytically tractable expressions for coverage and rates, which produce useful insights on network design guidance, have been found for ad-hoc [2], [3], cellular [4]–[7], multi-antenna [7], mmWave [8], and UAVs [9] networks.

Recently, PPPs have also been used to model the spatial distribution of satellites' placements in a portion on the surface of a sphere, i.e., a finite space. [16], [17], the downlink coverage probability of a satellite network is derived using the approximation of the contact angle distribution. In [13], the coverage and rate are analyzed for a noise-limited LEO satellite network by modeling satellites' locations according to a nonhomogeneous PPP with a non-uniform satellite intensity depending on latitudes. These prior works in [12], [13], [16]–[19] extend the realm of stochastic geometry into modeling satellite networks on the spherical cap. Notwithstanding the progress, the derived expressions for the coverage and rate are not very analytically tractable compared to the astonishingly simple expression on the coverage probability obtained in cellular networks, in which the base stations are randomly deployed according to a PPP in an infinite two-dimensional space [2]–[6].

This paper presents a novel framework for evaluating satellite downlink networks in a finite space.

- We first derive a new nearest distance distribution from a typical receiver's location to the satellite when distributed according to a PPP in a finite area, the surface of a sphere. Our key finding is that this conditional nearest distance distribution is a truncated variant of the time-honored nearest distance distribution called *Rayleigh distribution* of a PPP in an infinite space.
- We derive a tight lower and upper bound of the coverage probability in tractable forms in terms of system parameters, chiefly the path-loss exponent, the density, and the altitude of satellites. We further derive a tight lower bound of the coverage probability in closed form, which illuminates the features of the system parameters in the coverage probability.
- We identify the optimal density of the satellites for the typical user as a function of the satellite's height and the path-loss exponent. Our finding is that the optimal average number of satellites scales down as the altitude of satellites becomes higher. Furthermore, through simulations, the accuracy of the derived coverage probabilities is verified.

II. System Model

In this section, we explain the proposed network model and the performance metrics for the analysis of downlink satellite

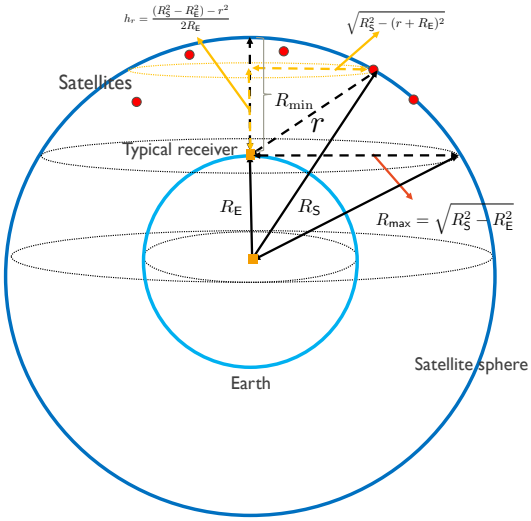

Fig. 1. Geometry of satellite networks. Satellites are assumed to be placed on the surface of a sphere with radius R_{S}. A typical receiver is located at $(0, 0, R_{\mathsf{E}})$. The distance from the typical receiver to a satellite r is calculated in terms of geometry parameters R_{S} and R_{E}.

networks.

The surface of a sphere in $\mathbb{R}^3$ with center at the origin $\mathbf{0} \in \mathbb{R}^3$ and fixed radius R_{S} is defined as

$$\mathbb{S}^2_{R_{\mathsf{S}}} = \{\mathbf{x} \in \mathbb{R}^3 : \|\mathbf{x}\|_2 = R_{\mathsf{S}}\}. \tag{1}$$

Let $\Phi = \{\mathbf{x}_1, \ldots, \mathbf{x}_N\}$ be a point process consisted of a finite number elements on the surface of a sphere $\mathbb{S}^2_{R_{\mathsf{S}}}$. Φ is said to a homogenous spherical Poisson point process (SPPP), provided that the number of points on $\mathbb{S}^2_{R_{\mathsf{S}}}$, $N = \Phi(\mathbb{S}^2_{R_{\mathsf{S}}})$, follows Poisson random variable with mean $\lambda|\mathbb{S}^2_{R_{\mathsf{S}}}| = 4\pi R^2\lambda$, namely,

$$\mathbb{P}\left(N = n\right) = \exp\left(-4\pi R^2\lambda\right)\frac{\left(4\pi R^2\lambda\right)^n}{n!}, \tag{2}$$

where $|\mathbb{S}^2_{R_{\mathsf{S}}}| = 4\pi R^2$ is the surface area of the sphere. For given N, the $\{\mathbf{x}_1, \ldots, \mathbf{x}_N\}$ forms a BPP, in which $\mathbf{x}_i$ for $i \in [N]$ is independent and uniformly distributed on the surface of the sphere.

We assume that the satellites are located on the surface of the sphere with radius R. The locations of them are distributed according to a homogeneous SPPP with density λ, i.e., $\Phi = \{\mathbf{x}_1, \ldots, \mathbf{x}_N\}$, where N follows a Poisson distribution with mean $4\lambda\pi R^2_{\mathsf{S}}$. Each SBS uses transmit power P. We further consider a collection of downlink users. Let $\mathbb{S}^2_{R_{\mathsf{E}}}$ be the surface of the Earth with the radius R_{E} ($< R_{\mathsf{S}}$). The locations of users on $\mathbb{S}^2_{R_{\mathsf{E}}}$ are assumed to be distributed according to a homogeneous SPPP with density λ_{U}, i.e., $\Phi_{\mathsf{U}} = \{\mathbf{u}_1, \ldots, \mathbf{u}_M\}$, where M follows a Poisson distribution with mean $4\lambda_{\mathsf{U}}\pi R^2_{\mathsf{E}}$. We assume that Φ_{U} is independent of underlying satellite BSs placement processes Φ.

Since we assume that both Φ and Φ_{U} are distributed according to the homogeneous SPPPs on $\mathbb{S}^2_{R_{\mathsf{S}}}$ and $\mathbb{S}^2_{R_{\mathsf{E}}}$, the satistical distribution of Φ with respect to any point in Φ_{U} is invariant under rotation in $\mathbb{R}^3$. Thanks to Slivnyak's theorem [**?**], without loss of generality, we consider a typical user located at $\mathbb{S}^2_{R_{\mathsf{E}}}$ in $(0, 0, R_{\mathsf{E}})$. As depicted in Fig. 1, we define a typical spherical cap $\mathcal{S} \subset \mathcal{S}_R$ in the field of view at the typical receiver's location. In other words, the typical spherical cap is the portion of sphere $\mathbb{S}^2_{R_{\mathsf{S}}}$ cut off by a tangent plane to sphere $\mathbb{S}^2_{R_{\mathsf{E}}}$ (the Earth) centered at $(0, 0, R_{\mathsf{E}})$. Applying Archimedes' Hat-Box Theorem, the area of the typical spherical cap is given by

$$|\mathcal{A}| = 2\pi(R_{\mathsf{E}} + R_{\mathsf{S}})R_{\mathsf{S}}. \tag{3}$$

Also, we define a spherical cap that contains the points with smaller distance than r from the typical location as

$$\mathcal{A}_r = \{\mathbf{x} \in \mathbb{S}^2_{R_{\mathsf{S}}} : \|\mathbf{x} - (0, 0, R_{\mathsf{E}})\|_2 \leq r\} \subset \mathcal{A}, \tag{4}$$

where $R_{\min} \leq r \leq R_{\max}$. Without loss of generality, we focus on a downlink user performance in the typical spherical cap.

A. SINR

We assume that the typical user is served by the nearest satellite. Let $\mathbf{x}_1 \in \Phi$ be the location of the nearest satellite, the signal-to-interference-puls-noise (SINR) experienced by the typical receiver located at $\mathbf{u}_1 = (0, 0, R_{\mathsf{E}})$ is:

$$\mathsf{SINR} = \frac{G_1 P H_1 \|\mathbf{x}_1 - \mathbf{u}_1\|^{-\alpha}}{\sum_{\mathbf{x}_i \in \Phi \cap \mathcal{S}/\{\mathbf{x}_1\}} G_i P H_i \|\mathbf{x}_i - \mathbf{u}_1\|^{-\alpha} + \sigma^2}, \tag{5}$$

where σ^2 denotes the noise power, H_i denotes fading power from satellite i to the receiver. We shall focus on the Nakagami-m fading distribution to model fading power H_i. Assuming $\mathbb{E}[H_i] = 1$, the probability density function (PDF) of H_i is:

$$f_{H_i}(x) = \frac{2m^m}{\Gamma(m)} x^{2m-1} \exp\left(-mx^2\right). \tag{6}$$

for $x \geq 0$. The Nakagami-m distribution is versatile. For instance, when $m = 1$ and $m = \frac{(K+1)^2}{2K+1}$, it resorts to the Rayleigh and Rician-K fading distributions, respectively.

We define the coverage probability averaged over all possible satellite base stations' geometries, namely,

$$\begin{aligned} &P^{\mathsf{cov}}_{\mathsf{SINR}}(\gamma; \lambda, \alpha, R_{\mathsf{S}}, m) \\ &= \mathbb{P}\left[\frac{H_1\|\mathbf{x}_1 - \mathbf{u}_1\|^{-\alpha}}{\sum_{\mathbf{x}_i \in \Phi \cap \mathcal{A}/\{\mathbf{x}_1\}} \bar{G}_i H_i \|\mathbf{x}_i - \mathbf{u}_1\|^{-\alpha} + \bar{\sigma}^2} \geq \gamma \middle| \Phi(\mathcal{A}) > 0\right] \\ &\times \mathbb{P}[\Phi(\mathcal{A}) > 0]. \end{aligned} \tag{7}$$

III. Coverage Probability Analysis

In this section, we first provide an exact expression for the coverage probability and then derive a upper and lower bound of the coverage probability in analytically tractable forms.

A. Statistical Properties

Before providing the general expressions for the coverage probability, we first introduce three vital statistical properties of PPPs on the surface of a sphere, which will be the foundation of our analysis in the sequel.

Lemma 1 (Satellite-available probability)**.** *The probability that any satellite is visible at the typical receiver is given by*

$$\mathbb{P}\left[\Phi(\mathcal{A})>0\right]=1-\exp\left(-\lambda 2\pi(R_{\mathsf{S}}-R_{\mathsf{E}})R_{\mathsf{S}}\right). \quad (8)$$

Proof. Since the locations of satellites follow PPPs on the surface of a sphere, it is sufficient to compute the probability that there is no satellites exists in a typical spherical cap $\mathcal{A}$, namely,

$$\begin{aligned}\mathbb{P}\left[\Phi(\mathcal{A})=0\right]&=\exp\left(-\lambda(|\mathcal{A}|)\right)\\&=\exp\left(-\lambda 2\pi(R_{\mathsf{S}}-R_{\mathsf{E}})R_{\mathsf{S}}\right),\end{aligned} \quad (9)$$

where $|\mathcal{A}|=2\pi(R_{\mathsf{S}}-R_{\mathsf{E}})R_{\mathsf{S}}$ is the Lebesgue measure of set $\mathcal{A}$ as in (3). ■

Lemma 2 (The conditional nearest satellite distance distribution)**.** *Let $R=\min_{\mathbf{x}_i\in\Phi\cap\mathcal{A}}\|\mathbf{x}_i-\mathbf{u}_1\|_2$ be the nearest distance from the typical user's location $\mathbf{u}_1=(0,0,R_{\mathsf{E}})$ to a satellite in $\Phi\cap\mathcal{A}$. Then, the PDF of R is*

$$f_{R|\Phi(\mathcal{A})>0}(r)=\begin{cases}\nu(\lambda,R_{\mathsf{S}})re^{-\lambda\pi\frac{R_{\mathsf{S}}}{R_{\mathsf{E}}}r^2} & \text{for } R_{\min}\le r\le R_{\max}\\ 0 & \text{otherwise,}\end{cases} \quad (10)$$

where $\nu(\lambda,R_{\mathsf{S}})=2\pi\lambda\frac{R_{\mathsf{S}}}{R_{\mathsf{E}}}\frac{e^{\lambda\pi\frac{R_{\mathsf{S}}}{R_{\mathsf{E}}}\left(R_{\mathsf{S}}^2-R_{\mathsf{E}}^2\right)}}{e^{2\lambda\pi R_{\mathsf{S}}(R_{\mathsf{S}}-R_{\mathsf{E}})}-1}$, $R_{\min}=R_{\mathsf{S}}-R_{\mathsf{E}}$, and $R_{\max}=\sqrt{R_{\mathsf{S}}^2-R_{\mathsf{E}}^2}$.

Proof. We compute the probability that the nearest neighbor of a point $\mathbf{x}_1\in\Phi$ is larger than r conditioned that at least more than one SBS exists in $\mathcal{A}$. To this end, we calculate the probability that there is no point in the area $\mathcal{A}_r$ as illustrated in Fig. 1, i.e., $\Phi(\mathcal{A}_r)=0$, conditioned $\Phi(\mathcal{A})>0$. Using Bayes' theorem, we compute

$$\begin{aligned}\mathbb{P}\left[R>r|\Phi(\mathcal{A})>0\right]&=\mathbb{P}[\Phi(\mathcal{A}_r)=0|\Phi(\mathcal{A})>0]\\&\overset{(a)}{=}\frac{\mathbb{P}[\Phi(\mathcal{A}_r)=0]\mathbb{P}[\Phi(\mathcal{A}/\mathcal{A}_r)>0]}{\mathbb{P}[\Phi(\mathcal{A})>0]}\\&\overset{(b)}{=}\frac{\exp\left(-\lambda|\mathcal{A}_r|\right)\left(1-\exp\left(-\lambda|\mathcal{A}/\mathcal{A}_r|\right)\right)}{1-\exp\left(-\lambda|\mathcal{A}|\right)}\\&=\frac{\exp\left(-\lambda|\mathcal{A}_r|\right)-\exp\left(-\lambda|\mathcal{A}|\right)}{1-\exp\left(-\lambda|\mathcal{A}|\right)},\end{aligned} \quad (11)$$

where (a) follows from the independence of the PPP for non-overlapping areas $\mathcal{A}/\mathcal{A}_r$ and $\mathcal{A}_r$ and (b) is by Lemma 1. To accomplish this, we need to compute the area of a spherical cap $\mathcal{A}_r$. By the Archimedes' Hat-Box Theorem, the area of $\mathcal{A}_r$ is given by

$$|\mathcal{A}_r|=2\pi(R_{\mathsf{S}}-R_{\mathsf{E}}-h_r)R_{\mathsf{S}}. \quad (12)$$

Using Pythagoras theorem as depicted in Fig. 1, we can express h_r in terms of r as $h_r=\frac{(R_{\mathsf{S}}^2-R_{\mathsf{E}}^2)-r^2}{2R_{\mathsf{E}}}$ Invoking above equation into (12), the area of $\mathcal{A}_r$ is represented as

$$|\mathcal{A}_r|=2\pi\left(R_{\mathsf{S}}-R_{\mathsf{E}}-\frac{(R_{\mathsf{S}}^2-R_{\mathsf{E}}^2)-r^2}{2R_{\mathsf{E}}}\right)R_{\mathsf{S}}. \quad (13)$$

As a result, the probability that no satellite exists in $\mathcal{A}_r$ is $\mathbb{P}\left[\Phi(\mathcal{A}_r)=0\right]=e^{-2\lambda\pi R_{\mathsf{S}}(R_{\mathsf{S}}-R_{\mathsf{E}})}e^{-\lambda\pi\frac{R_{\mathsf{S}}}{R_{\mathsf{E}}}\left\{r^2-(R_{\mathsf{S}}^2-R_{\mathsf{E}}^2)\right\}}$ Also, the probability that there is no satellite in $\mathcal{A}$ is computed as

$$\mathbb{P}\left[\Phi(\mathcal{A})=0\right]=e^{-2\lambda\pi R_{\mathsf{S}}(R_{\mathsf{S}}-R_{\mathsf{E}})}. \quad (14)$$

Plugging these into (11), we obtain the conditional CCDF of R

$$F^{c}_{R|\Phi(\mathcal{A})>0}(r)=\frac{e^{-2\lambda\pi R_{\mathsf{S}}(R_{\mathsf{S}}-R_{\mathsf{E}})}\left[e^{-\lambda\pi\frac{R_{\mathsf{S}}}{R_{\mathsf{E}}}\left\{r^2-(R_{\mathsf{S}}^2-R_{\mathsf{E}}^2)\right\}}-1\right]}{1-e^{-2\lambda\pi R_{\mathsf{S}}(R_{\mathsf{S}}-R_{\mathsf{E}})}}. \quad (15)$$

By taking derivative with respect to r, we obtain the conditional distribution of the nearest satellite distance as in (10). ■

Lemma 3. *The conditional Laplace transform of the aggregated interference is*

$$\begin{aligned}&\mathcal{L}_{I_r|\Phi(\mathcal{A})>0}(s)\\&=\exp\left(-\lambda\pi\frac{R_{\mathsf{S}}}{R_{\mathsf{E}}}\left(\frac{\bar{G}_i s}{m}\right)^{\frac{2}{\alpha}}\int_{\left(\frac{\bar{G}_i s}{m}\right)^{-\frac{2}{\alpha}}r^2}^{R_{\max}^2}1-\frac{1}{\left(1+u^{-\frac{\alpha}{2}}\right)^m}\mathrm{d}u\right).\end{aligned} \quad (16)$$

Proof. We omit the proof due to the space limitation. We refer to the proof in our journal version [20]. ■

B. Upper and Lower Bounds

We provide an upper and lower bound of the coverage probability expression, while keeping full generality.

Theorem 1. *The coverage probability in the interference-limited regime is upper and lower bounded as*

$$\begin{aligned}P_{\mathsf{SIR}}^{\mathrm{cov,B}}(\gamma;\lambda,\alpha,R_{\mathsf{S}},m,\kappa^{\mathrm{L}})&\le P_{\mathsf{SIR}}^{\mathrm{cov}}(\gamma;\lambda,\alpha,R_{\mathsf{S}},m)\\P_{\mathsf{SIR}}^{\mathrm{cov}}(\gamma;\lambda,\alpha,R_{\mathsf{S}},m)&\le P_{\mathsf{SIR}}^{\mathrm{cov,B}}(\gamma;\lambda,\alpha,R_{\mathsf{S}},m,\kappa^{\mathrm{U}})\end{aligned} \quad (17)$$

with $\kappa^{\mathsf{U}}=1$, $\kappa^{\mathsf{U}}=m!^{-\frac{1}{m}}$, and

$$\begin{aligned}&P_{\mathsf{SIR}}^{\mathrm{cov,B}}(\gamma;\lambda,\alpha,R_{\mathsf{S}},m,\kappa)\\&=2\pi\lambda\frac{R_{\mathsf{S}}}{R_{\mathsf{E}}}e^{\lambda\pi\frac{R_{\mathsf{S}}}{R_{\mathsf{E}}}(R_{\mathsf{S}}-R_{\mathsf{E}})^2}\sum_{\ell=1}^{m}\binom{m}{\ell}(-1)^{\ell+1}\\&\quad\times\int_{R_{\min}}^{R_{\max}}re^{-\lambda\frac{R_{\mathsf{S}}}{R_{\mathsf{E}}}\pi[1+\eta(\ell m\kappa\gamma,r;\alpha,R_{\mathsf{S}},m)]r^2}\mathrm{d}r,\end{aligned} \quad (18)$$

where $\kappa\in\{1,m!^{-\frac{1}{m}}\}$ and

$$\begin{aligned}&\eta(x,r;\alpha,R_{\mathsf{S}},m)\\&=\left(\frac{\bar{G}_i x}{m}\right)^{\frac{2}{\alpha}}\int_{\left(\frac{\bar{G}_i x}{m}\right)^{-\frac{2}{\alpha}}}^{\left(\frac{R_{\max}}{r}\right)^2}1-\frac{1}{\left(1+u^{-\frac{\alpha}{2}}\right)^m}\mathrm{d}u.\end{aligned} \quad (19)$$

Proof. We devote to proving the upper bound, since the lower bound is readily obtained from the former by choosing $\kappa=1$. Conditioned on the nearest satellite being placed at distance r

from the typical receiver's location, the conditional probability can be written as

$$P^{\text{cov}}_{\mathsf{SIR}|\Phi(\mathcal{A})>0}(\gamma;\lambda,\alpha,R_{\mathsf{S}},m) = \mathbb{E}\left[\mathbb{P}\left[H_1 \geq r^{\alpha}\gamma I_r \mid \Phi(\mathcal{A})>0, R_1=r\right] \mid \Phi(\mathcal{A})>0\right]. \tag{20}$$

Recall that the CCDF for H_1 can be represented in terms of the lower incomplete gamma function as

$$\mathbb{P}[H_1 > x] = 1 - \frac{1}{\Gamma(m)}\int_0^{mx} t^{m-1}e^{-t}\mathrm{d}t. \tag{21}$$

From the Alzer's inequality [21], the incomplete Gamma function has an expression in the middle sandwiched between two inequalities:

$$\left(1-e^{-m\kappa x}\right)^m \leq \frac{1}{\Gamma(m)}\int_0^{mx} t^{m-1}e^{-t}\mathrm{d}t \leq \left(1-e^{-mx}\right)^m. \tag{22}$$

Using this, the CCDF for H_1 is upper and lower bounded by

$$\left(1-e^{-mx}\right)^m \leq \mathbb{P}[H_1 > x] \leq \left(1-e^{-m\kappa x}\right)^m, \tag{23}$$

where $\kappa = (m!)^{-\frac{1}{m}}$ and the equality holds when $m=1$. Applying the binomial expansion

$$1-\left(1-e^{-m\kappa x}\right)^m = \sum_{\ell=1}^{m}\binom{m}{\ell}(-1)^{\ell+1}e^{-\ell m\kappa x}$$

and plugging (21) into (20), we obtain an upper bound of the conditional coverage probability as

$$\begin{aligned} &P^{\text{cov}}_{\mathsf{SIR}|\Phi(\mathcal{A})>0}(\gamma;\lambda,\alpha,R_{\mathsf{S}},m) \\ &\leq \sum_{\ell=1}^{m}\binom{m}{\ell}(-1)^{\ell+1} \\ &\quad\times \mathbb{E}\left[\mathbb{E}\left[e^{-\ell m\kappa r^{\alpha}\gamma I_r} \mid R_1=r, \Phi(\mathcal{A})>0\right] \mid \Phi(\mathcal{A})>0\right] \\ &= \sum_{\ell=1}^{m}\binom{m}{\ell}(-1)^{\ell+1}\mathbb{E}\left[\mathcal{L}_{I_r|\Phi(\mathcal{A})>0}\left(\ell m\kappa r^{\alpha}\gamma\right) \mid \Phi(\mathcal{A})>0\right], \end{aligned} \tag{24}$$

where the remaining expectation is taken over the distribution of $f_{R|\Phi(\mathcal{A})}(r)$ in Lemma 2. Toward this end, we compute the conditional Laplace transform of the aggregated interference power. From the Lemma 3, such Laplace transform is

$$\begin{aligned} &\mathcal{L}_{I_r|\Phi(\mathcal{A})>0}(\ell m\kappa r^{\alpha}\gamma) \\ &= \exp\left(-\lambda\pi\frac{R_{\mathsf{S}}}{R_{\mathsf{E}}}r^2\eta(\ell m\kappa\gamma, r;\alpha,R_{\mathsf{S}},m)\right). \end{aligned} \tag{25}$$

Invoking (25) into (24) and computing the expectation with respect to the nearest distance distribution given in Lemma 2, we obtain $P^{\text{cov}}_{\mathsf{SIR}|\Phi(\mathcal{A})>0}(\gamma;\lambda,\alpha,R_{\mathsf{S}},m)$. Multiplying $\mathbb{P}[\Phi(\mathcal{A})>0] = 1-e^{-\lambda 2\pi(R_{\mathsf{S}}-R_{\mathsf{E}})R_{\mathsf{S}}}$ to the conditional coverage probability, we arrive at the expression in (26), which completes the proof. ■

As illustrated in Fig. 2, the derived coverage probability expression in (18) tightly matches with the exact coverage probability obtained via numerical simulations over the entire range of γ of interest and for the values of all relevant system parameters, λ, α, m, and R_{S}.

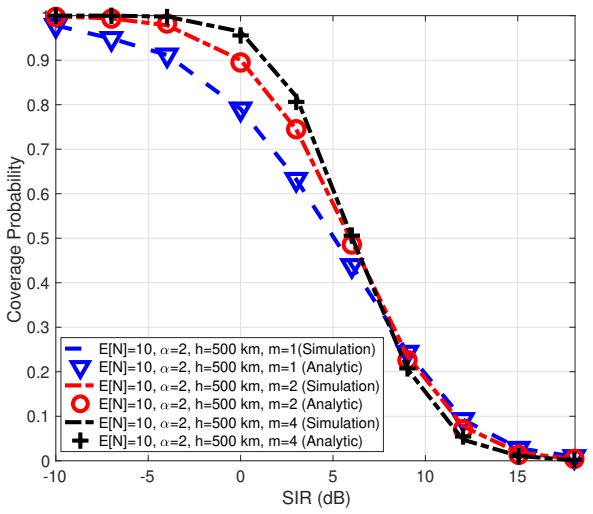

Fig. 2. The coverage probability according to the Nakagami fading parameter $m \in \{1,2,4\}$ for fixed $\alpha=2$ and $\lambda|\mathcal{S}|=10$ with $\kappa=\{1,0.51,0.71\}$, respectively.

C. Lower Bound in Closed-From

To make the analysis more tractable, we characterize the lower bound for the coverage probability in closed form. Our approach to derive the lower bound is to represent the integral term in the conditional Laplace in Lemma 3 to be independent of r, while making this tight. The following corollary represents a lower bound of the coverage probability in Theorem 1 in closed-form.

Corollary 1. *A lower bound of the coverage probability in closed from is given by*

$$\begin{aligned} &P^{\text{cov,L}}_{\mathsf{SIR}}(\gamma;\lambda,\alpha,R_{\mathsf{S}},m) \\ &= \sum_{\ell=1}^{m}\binom{m}{\ell}(-1)^{\ell+1}\left[\frac{e^{-\lambda\pi\frac{R_{\mathsf{S}}}{R_{\mathsf{E}}}\eta^{\mathsf{U}}(\ell m\gamma;\alpha,R_{\mathsf{S}},m)R_{\min}^2}}{1+\eta^{\mathsf{U}}(\ell m\gamma;\alpha,R_{\mathsf{S}},m)}\right. \\ &\qquad\left. - \frac{e^{-\lambda\pi\frac{R_{\mathsf{S}}}{R_{\mathsf{E}}}\left[\left\{1+\eta^{\mathsf{U}}(\ell m\gamma;\alpha,R_{\mathsf{S}},m)\right\}R_{\max}^2-R_{\min}^2\right]}}{1+\eta^{\mathsf{U}}(\ell m\gamma;\alpha,R_{\mathsf{S}},m)}\right], \end{aligned} \tag{26}$$

where

$$\begin{aligned} &\eta^{\mathsf{U}}(x;\alpha,R_{\mathsf{S}},m) \\ &= \left(\frac{\bar{G}_i x}{m}\right)^{\frac{2}{\alpha}}\int_{\left(\frac{\bar{G}_i x}{m}\right)^{-\frac{2}{\alpha}}}^{\left(\frac{R_{\max}}{R_{\min}}\right)^2} 1-\frac{1}{\left(1+u^{-\frac{\alpha}{2}}\right)^m}\mathrm{d}u. \end{aligned} \tag{27}$$

Proof. The proof is direct from the marginalization of (24) with respect to $f_{R|\Phi(\mathcal{A})>0}(r)$ and the inequality $\eta^{\mathsf{U}}(x;\alpha,R_{\mathsf{S}},m) \geq \eta(x,r;\alpha,R_{\mathsf{S}},m)$ since $R_{\min} \leq r \leq R_{\max}$. ■

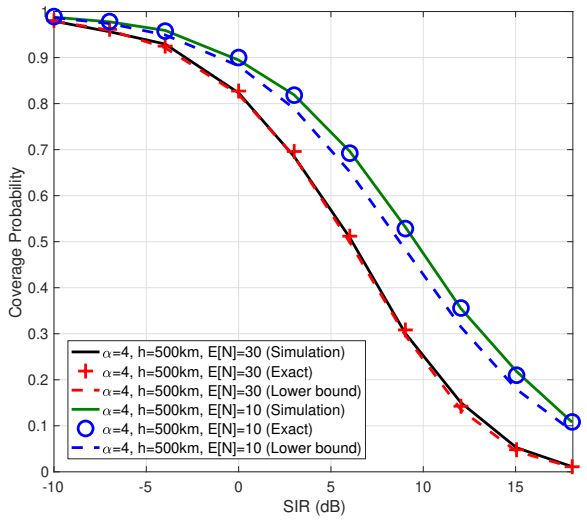

Fig. 3. The coverage probability according to the satellite density for fixed $\alpha = 4$ and $m = 1$.

From the derived lower bound of the coverage probability, we can see that the coverage probability changes over the density of satellites λ for fixed path-loss exponent α, satellites' altitude R_{S}, and target threshold γ. This result is in contrast to the coverage probability for terrestrial cellular networks modeled by homogenous PPPs, in which the coverage probability has shown to be invariant with the density of base stations in the interference-limited regime [4], [7].

It is remarkable that the coverage probability can be either increase or decrease depending on the satellite density λ. As the density becomes smaller, the conditional coverage probability $P^{\mathrm{cov,L}}_{\mathsf{SIR}|\Phi(\mathcal{A})>0}(\gamma;\lambda,\alpha,R_{\mathsf{S}},m)$ improves, while the satellite available probability $\mathbb{P}[\Phi(\mathcal{A})>0] = \left(1-e^{-\lambda 2\pi(R_{\mathsf{S}}-R_{\mathsf{E}})R_{\mathsf{S}}}\right)$ becomes deteriorated. As a result, optimizing the satellite density is the key to maximize the coverage performance in the satellite network design. In the next section, we will characterize the optimal satellite density for given other network design parameters.

Fig. 3 shows the tightness of the derived lower bound for the coverage probability in Corollary 1. The lower bound becomes tight as the density of satellites increases. When the density is high, the difference between $\eta(\gamma;\alpha,R_{\mathsf{S}},1)$ and $\eta^{\mathsf{U}}(\gamma;\alpha,R_{\mathsf{S}},1)$ becomes less significant to the coverage probability.

IV. Optimal Satellite Density

In this section, we derive an optimal satellite density that maximizes the lower bound of the coverage probability in Corollary 1. The following theorem illuminates how the optimal satellite density is determined as a function of satellite height $R_{\min}$ and path-loss exponent α.

Theorem 2. *For given α, $R_{\mathsf{S}} = R_{\min} + R_{\mathsf{E}}$, and γ, we define the optimal density that maximizes the lower bound of the coverage probability as*

$$\lambda^{\star} = \arg\max_{\lambda\geq 0} P^{\mathrm{cov,L}}_{\mathsf{SIR}}(\gamma;\lambda,\alpha,R_{\mathsf{S}},1). \tag{28}$$

Then, such optimal density is

$$\lambda^{\star} = \frac{\ln\left(1+\frac{2(1+\eta^{\mathsf{U}}(\gamma;\alpha,R_{\mathsf{S}},1))R_{\mathsf{E}}}{\eta^{\mathsf{U}}(\gamma;\alpha,R_{\mathsf{S}},1)R_{\min}}\right)}{2\pi\left[1+\eta^{\mathsf{U}}(\gamma;\alpha,R_{\mathsf{S}},1)\right]R_{\min}(R_{\mathsf{E}}+R_{\min})}. \tag{29}$$

Proof. For notational simplicity, we let $a = \pi\frac{R_{\mathsf{S}}}{R_{\mathsf{E}}}\eta^{\mathsf{U}}(\gamma;\alpha,R_{\mathsf{S}},1)R^2_{\min}$, $b = \pi\frac{R_{\mathsf{S}}}{R_{\mathsf{E}}}\left[\left(1+\eta^{\mathsf{U}}(\gamma;\alpha,R_{\mathsf{S}},1)\right)R^2_{\max}-R^2_{\min}\right]$, and $c = 1+\eta^{\mathsf{U}}(\gamma;\alpha,R_{\mathsf{S}},1)$. Then, the lower bound of the coverage probability in (26), can be expressed as

$$P^{\mathrm{cov,L}}_{\mathsf{SIR}}(\gamma;\lambda,\alpha,R_{\mathsf{S}},1) = \frac{e^{-a\lambda}-e^{-b\lambda}}{c}, \tag{30}$$

where $0<a<b$ and $0<c$. From (30), we notice that $P^{\mathrm{cov,L}}_{\mathsf{SIR}}(\gamma;\lambda,\alpha,R_{\mathsf{S}},1)$ is a neither convex nor concave function with respect to any positive value of λ. Therefore, to verify the existence and the uniqueness of $\lambda^{\star}$, we first need to show that $P^{\mathrm{cov,L}}_{\mathsf{SIR}}(\gamma;\lambda,\alpha,R_{\mathsf{S}},1)$ is unimodal function with respect to $\lambda>0$. Toward this end, a manipulation deduces that $P^{\mathrm{cov,L}}_{\mathsf{SIR}}(\gamma;\lambda,\alpha,R_{\mathsf{S}},1)$ is increasing on $\lambda\in[0,\lambda^{\star}]$ and decreasing on $[\lambda^{\star},\infty)$:

$$\begin{aligned}&\frac{\partial P^{\mathrm{cov,L}}_{\mathsf{SIR}}(\gamma;\lambda,\alpha,R_{\mathsf{S}},1)}{\partial\lambda} > 0\\ &\Leftrightarrow \lambda > \frac{\ln\left(\frac{b}{a}\right)}{b-a} = \lambda^{\star}.\end{aligned} \tag{31}$$

By virtue of the unimodality of $P^{\mathrm{cov,L}}_{\mathsf{SIR}}(\gamma;\lambda,\alpha,R_{\mathsf{S}},1)$, $P^{\mathrm{cov,L}}_{\mathsf{SIR}}(\gamma;\lambda,\alpha,R_{\mathsf{S}},1)$ has a unique maximum at $\lambda=\lambda^{\star}$. Plugging the definitions of a, b, and c into (31), the optimal density for given network parameters is given by

$$\lambda^{\star} = \frac{\ln\left(\frac{\left[1+\eta^{\mathsf{U}}(\gamma;\alpha,R_{\mathsf{S}},1)\right]R^2_{\max}-R^2_{\min}}{\eta^{\mathsf{U}}(\gamma;\alpha,R_{\mathsf{S}},1)R^2_{\min}}\right)}{\pi\frac{R_{\mathsf{S}}}{R_{\mathsf{E}}}\left[1+\eta^{\mathsf{U}}(\gamma;\alpha,R_{\mathsf{S}},1)\right]\left(R^2_{\max}-R^2_{\min}\right)}. \tag{32}$$

Using relation of $R^2_{\max} = (R_{\min}+2R_{\mathsf{E}})R_{\min}$, we arrive at the expression in (29), which completes the proof. ■

Theorem 2 suggests that the optimal density $\lambda^{\star}$ diminishes as the altitude of the satellite $R_{\min}$ increases. This result implies that it is necessary to deploy more satellites for VLEO networks to enhance the coverage performance, which agrees with the conventional wisdom obtained from extensive simulation studies [11].

To provide a better understanding the result in Theorem 2, it is more informative to characterize the optimal average number of satellites by multiplying $\lambda^{\star}$ to the area of the spherical cap, namely,

$$\mathbb{E}[N^{\star}] = \frac{\ln\left(1+\frac{2(1+\eta^{\mathsf{U}}(\gamma;\alpha,R_{\mathsf{S}},1))R_{\mathsf{E}}}{\eta^{\mathsf{U}}(\gamma;\alpha,R_{\mathsf{S}},1)R_{\min}}\right)}{2\pi\left[1+\eta^{\mathsf{U}}(\gamma;\alpha,R_{\mathsf{S}},1)\right]}. \tag{33}$$

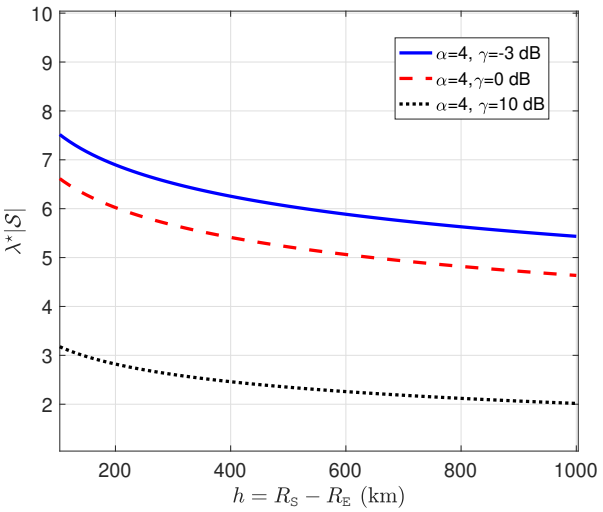

Fig. 4. The optimal mean number of satellites versus the altitude of satellites according to the target threshold γ for fixed $\alpha = 4$ and $m = 1$.

This fact elucidates the optimal trade-off between the average number of satellites and altitude $R_{\min}$. From this trade-off, we can provide valuable guidance in the network design. For instance, the average number of satellites in the typical spherical cap scales down with the altitude logarithmically to maximize the coverage performance. In particular, for VLEO satellite networks, in which $R_{\min} \ll R_{\mathsf{E}} (= 6350 \text{ km})$, the optimal number of satellites approximately boils down to

$$\mathbb{E}[N^\star] \simeq \frac{R_{\mathsf{E}}}{\pi \eta^{\mathsf{U}}(\gamma; \alpha, R_{\mathsf{S}}, 1) R_{\min}}. \tag{34}$$

In the shallow altitude regime, that average number of satellites can scale down linearly with the altitude. Nonetheless, deploying more satellites requires high costs; a satellite network operator needs to optimize the trade-off between the deploying cost and the coverage performance.

Optimal trade-off: Fig. 4 shows the optimal trade-off between the average number of satellites $\lambda^\star|\mathcal{S}|$ and the satellite altitude $h = R_{\mathsf{S}} - R_{\mathsf{E}}$ derived in (33). As can be seen, the optimal average number scales down logarithmically with the altitude. This trade-off suggests that a network operator must carefully choose a satellite density depending on the network altitude.

V. Conclusion

In this paper, we have characterized the coverage performance of satellite networks. Using stochastic geometry tools, we have derived the coverage probability in terms of the satellite density, the Nakagami fading parameter, and the path-loss exponent. From these obtained analytical expressions, we have shown that the LOS propagation is beneficial to reduce the fading effects, while it is less preferred due to high co-channel interference effects. More importantly, we have found that the optimal mean number of satellites for maximizing the coverage probability and the number scales down logarithmically as the satellite altitude increases.

References

[1] S. Liu, Z. Gao, Y. Wu, D. W. Kwan Ng, X. Gao, K.-K. Wong, S. Chatzinotas, and B. Ottersten, "LEO satellite constellations for 5G and beyond: How will they reshape vertical domains?," *in IEEE Communications Magazine,* vol. 59, no. 7, pp. 30–36, 2021.

[2] F. Baccelli, B. Blaszczyszyn, and P. Muhlethaler, "An ALOHA protocol for multihop mobile wireless networks," *in IEEE Trans. Inform. Theory,* vol. 52, no. 2, pp. 421-436, Feb. 2006.

[3] M. Haenggi, "A geometric interpretation of fading in wireless networks: Theory and applications," *in IEEE Trans. Inf. Theory,* vol. 54, no. 12, pp. 5500–5510, Dec. 2008.

[4] J. G. Andrews, F. Baccelli, and R. K. Ganti, "A tractable approach to coverage and rate in cellular networks," *in IEEE Trans. Commun.,* vol. 59, no. 11, pp. 3122 – 3134, Nov. 2011.

[5] H. S. Dhillon, R. K. Ganti, F. Baccelli and J. G. Andrews, "Modeling and analysis of K-tier downlink heterogeneous cellular networks," *in IEEE J. Sel. Areas Commun.,* vol. 30, no. 3, pp. 550–560, April 2012.

[6] N. Lee, X. Lin, J. G. Andrews and R. W. Heath, "Power control for D2D underlaid cellular networks: modeling, algorithms, and analysis," *in IEEE J. Sel. Areas Commun.,* vol. 33, no. 1, pp. 1–13, Jan. 2015.

[7] N. Lee, D. Morales-Jimenez, A. Lozano and R. W. Heath, "Spectral efficiency of dynamic coordinated beamforming: A stochastic geometry approach," *in IEEE Trans. Wireless Commun.,* vol. 14, no. 1, pp. 230–241, Jan. 2015.

[8] T. Bai, A. Alkhateeb, and R. W. Heath, Jr., "Coverage and capacity of millimeter wave cellular networks," *in IEEE Communications Magazine.* vol. 52, no. 9, pp. 70-77, Sept. 2014.

[9] V. V. Chetlur and H. S. Dhillon, "Downlink coverage analysis for a finite 3-D wireless network of unmanned aerial vehicles," *in IEEE Trans. Commun,* vol. 65, no. 10, pp. 4543–4558, Jul. 2017.

[10] A. Ganz, Y. Gong, and B. Li, "Performance study of low Earth-orbit satellite systems," *in IEEE Trans. Commun.,* vol. 42, no. 234, pp. 1866–1871, Feb. 1994.

[11] F. Vatalaro, G. E. Corazza, C. Caini, and C. Ferrarelli, "Analysis of LEO, MEO, and GEO global mobile satellite systems in the presence of interference and fading," *in IEEE J. Sel. Areas Commun.,* vol. 13, no. 2, pp. 291–300, Feb. 1995.

[12] N. Okati, T. Riihonen, D. Korpi, I. Angervuori, and R. Wichman, "Downlink coverage and rate analysis of low Earth orbit satellite constellations using stochastic geometry," *in IEEE Trans. Commun.,* vol. 68, no. 8, pp. 5120–5134, Aug. 2020.

[13] N. Okati, T. Riihonen, "Modeling and analysis of LEO mega-constellations as nonhomogeneous Poisson point processes," *in Proc. IEEE 93rd Vehicular Technology Conference,* Apr. 2021.

[14] M. Haenggi, "On distances in uniformly random networks," *in IEEE Trans. Inform. Theory,* vol. 51, no. 10, pp. 3584 – 3586, Oct. 2005.

[15] M. Afshang and H. S. Dhillon, "Fundamentals of modeling finite wireless networks using binomial point process," *in IEEE Trans. Wireless Commun.,* vol. 16, no. 5, pp. 3355–3370, May 2017.

[16] A. Al-Hourani, "An analytic approach for modeling the coverage performance of dense satellite networks," *in IEEE Wireless Commun. Lett.,* vol. 10, no. 4, pp. 897–901, 2021.

[17] A. Al-Hourani, "Optimal satellite constellation altitude for maximal coverage," *in IEEE Commun. Lett.,* vol. 10, no. 7, pp. 1444–1448, 2021.

[18] A. Talgat, M. A. Kishk, and M.-S. Alouini, "Nearest neighbor and contact distance distribution for binomial point process on spherical surfaces," *in IEEE Commun. Lett.,* vol. 24, no. 12, pp. 2659–2663, 2020.

[19] A. Talgat, M. A. Kishk, and M.-S. Alouini, "Stochastic geometry-based analysis of LEO satellite communication systems," *in IEEE Commun. Lett.,* vol. 25, no. 8, pp. 2458–2462, 2021.

[20] J. Park, J. Choi, and N. Lee, "Coverage and spectral efficiency analysis for satellite downlink networks," *submitted to IEEE Trans. Wireless Commun.,* Nov. 2011.

[21] H. Alzer, "On some inequalities for the incomplete Gamma function," *in Math. Comput.,* vol. 66, no. 218, pp. 771 - 778, 2005.